ISSN 1063-7834, Physics of the Solid State, 2019, Vol. 61, No. 10, pp. 1904–1909. © Pleiades Publishing, Ltd., 2019.
Russian Text © The Author(s), 2019, published in Fizika Tverdogo Tela, 2019, Vol. 61, No. 10, pp. 1941–1947.

PHYSICS OF SURFACE AND THIN FILMS

Structural, Optical, and Thermoelectric Properties of the ZnO:Al Films Synthesized by Atomic Layer Deposition

I. A. Tambasov[a, *], M. N. Volochaev[a], A. S. Voronin[b], N. P. Evsevskaya[a, c], A. N. Masyugin[d], A. S. Aleksandrovskii[a, e], T. E. Smolyarova[b, e], I. V. Nemtsev[a], S. A. Lyashchenko[a], G. N. Bondarenko[c], and E. V. Tambasova[d]

[a] *Kirensky Institute of Physics, Krasnoyarsk Scientific Center, Siberian Branch, Russian Academy of Sciences, Krasnoyarsk, 660036 Russia*

[b] *Krasnoyarsk Scientific Center, Siberian Branch, Russian Academy of Sciences, Krasnoyarsk, 660036 Russia*

[c] *Institute of Chemistry and Chemical Technology, Krasnoyarsk Scientific Center, Siberian Branch, Russian Academy of Sciences, Krasnoyarsk, 660036 Russia*

[d] *Siberian State University of Science and Technology, Krasnoyarsk, 660014 Russia*

[e] *Siberian Federal University, Krasnoyarsk, 660041 Russia*

**e-mail: tambasov_igor@mail.ru*

Received April 15, 2019; revised April 15, 2019; accepted April 17, 2019

Abstract—Aluminum-doped zinc oxide thin films have been grown by atomic layer deposition at a temperature of 200°C. Using X-ray diffraction, it has been established that the ZnO:Al thin films exhibits the reflections from the (100), (002), (110), and (201) ZnO hexagonal phase planes. The (101) and (102) planes have also been detected by electron diffraction. The ZnO:Al thin films grow smooth with a root-mean-square roughness of $R_q = 0.33$ nm and characteristic nanocrystallite sizes of ~70 and ~15 nm without additional aluminum or aluminum oxide phases. The transmission at a wavelength of 550 nm with regard to the substrate has been found to be 96%. The refractive indices and absorption coefficients of the ZnO:Al thin films in the wavelength range of 250–900 nm have been determined. The maximum refractive indices and absorption coefficients have been found to be 2.09 at a wavelength of 335 nm and 0.39 at a wavelength of 295 nm, respectively. The optical band gap is 3.56 eV. The resistivity, Seebeck coefficient, and power factor of the ZnO:Al thin films are $\sim 1.02 \times 10^{-3}$ Ω cm, –60 μV/K, and 340 μW m^{-1} K^{-2} at room temperature, respectively. The maximum power factor attains 620 μW m^{-1} K^{-2} at a temperature of 200°C.

Keywords: atomic layer deposition, thin films, aluminum-doped zinc oxide, structural and optical properties, thermoelectric properties

DOI: 10.1134/S1063783419100354

1. INTRODUCTION

At present, the In_2O_3, ZnO, TiO_2, and other transparent conductive oxides are intensively investigated [1–6], since they possess simultaneously the ~90% transparency in the visible range and the ability to conduct electric current [1, 5, 6]. In most cases, the conductive oxides are used in the form of films with a thickness from several dozen to hundreds of nanometers.

The above-mentioned oxides are used in production of thin displays, organic, and inorganic light-emitting diodes, solar cells, thin-film transistors, gas sensors, etc. [1, 7–11]. These oxides are usually doped with donor atoms to increase their electrical conductivity via an increase in the electron density [12]. Today, one of the conductive oxides most highly sought in industry is In_2O_3 doped with Sn atoms (ITO) [13]. However, the steady increase in indium prices stimulates the search for and investigations of alternative materials that would be not inferior to ITO in their electrical and optical properties. One of the main alternatives is aluminum-doped zinc oxide ZnO:Al [14].

Currently, there exist different techniques for synthesizing the transparent conductive oxides, e.g., thermal vacuum deposition, magnetron sputtering, pulsed laser deposition, vapor-phase deposition, atomic layer deposition, and sol-gel process [15]. The donor impurity is conventionally activated by heating a substrate to 500°C [16]. This causes certain technological difficulties of thin film synthesis in view of the development of opto-, micro-, and nanoelectronics on polymer substrates sensitive to high processing temperatures [10, 16]. Therefore, reducing the processing temperature during the thin film synthesis is an urgent applied problem.

The transparent conductive oxides are currently considered also as thermoelectric materials [17]. Here, the key properties are the high electronic conductivity σ (S m^{-1}), the high Seebeck coefficient S (V K^{-1}), and the lowest thermal conductivity κ (W m^{-1} K^{-1}) of the materials [18]. A common integral characteristic of thermoelectric materials is the thermoelectric figure of merit $ZT = (S^2\sigma/\kappa)T$, where T is the mean temperature between the hot and cold sides of a thermoelectric converter. However, the investigations showed that the transparent conductive oxides with the high thermoelectric properties should be nanostructured [17], since this makes it possible to control the thermoelectric figure of merit due to structural features [19–21]. In particular, an important issue in the nanostructured thermoelectric materials is heat transfer. The structural features can work as thermal phonon scattering centers, thereby reducing the thermal conductivity coefficient [22]; ultimately, the thermoelectric figure of merit grows [22].

Thus, it is possible to implement several functional properties, including the electrical conductivity, high optical transparency, and thermoelectric properties, in one material. The transparent conductive oxide thin films possessing the above-listed properties can be used in transparent electronics as power sources placed on a transparent carrier [23]. The works on creating the alternative transparent conductive materials by low-temperature techniques and examining their physical, including thermoelectric, properties are of great importance.

In this study, we synthesized the ZnO:Al thin films by atomic layer deposition and explored their structural, optical, and thermoelectric properties.

2. EXPERIMENTAL

The ZnO:Al thin films were synthesized by atomic layer deposition on a Picosun R200 facility. Single-crystal silicon and AGC display glass were used as substrates. The precursors were diethylzinc $Zn(C_2H_5)_2$ (99.999%), trimethylaluminum $Al(CH_3)_3$ (purity 99.999%), and deionized aqueous vapor H_2O. The carrier gas was N_2 (99.9999%). Doping was performed during the growth using one $Al(CH_3)_3 + H_2O$ growth cycle per every twenty $Zn(C_2H_5)_2 + H_2O$ growth cycles. Thus, the maximum doping was about 5 at % of Al. The pulse length for each gas precursor was 0.1 s. The duration of each nitrogen purge of a chamber after a precursor was 4 s. The substrate temperature during the ZnO:Al thin film growth was 200°C. The technique for growing and doping the ZnO thin films was described in detail in [14, 24, 25].

The surface morphology of the thin films was examined on a Hitachi S5500 scanning electron microscope and a Nanoink DPN 5000 atomic force microscope. The thickness and microstructure of the ZnO:Al thin films were studied on a Hitachi TM7700 transmission electron microscope at an accelerating voltage of 100 kV in the cross sectional imaging mode [26, 27]. Cross sections were prepared by a focused ion beam technique on a Hitachi FB2100 facility with a liquid-metal Ga^+ ion source at an accelerating voltage of 40 kV. The ion plasma finishing was made on a Linda Technoorg Unimill pro 4 facility with Ar^+ ions at an accelerating voltage of 2 kV. The X-ray structural analysis of the synthesized films was performed on a DRON-4-07 diffractometer (CuK_α radiation).

The optical properties of the thin films were studied using a Shimadzu UV-3600 spectrometer and an Ellips-1891 spectral ellipsometer.

Silver contact pads were formed using an Emitech k575x vacuum unit. The contact thickness was ~500 nm. The thermoelectric properties (the Seebeck coefficient and electrical resistance) of the thin films at temperatures from room to 200°C were measured using an original setup consisting of a thermostat, a Keithley 2400 precision current source, a specially developed sample holder, which sets the sample heating gradient, two type-K thermocouples, and an LTR114 24-bit A/D converter, based on an LTR-EU-2 crate (L Card, Russia). The setup and thermoelectric measurement methods were described in detail in [28].

3. RESULTS AND DISCUSSION

The phase composition of the synthesized ZnO:Al thin films was determine by X-ray diffraction. Figure 1 shows the X-ray diffraction pattern of the ZnO:Al thin film. It can be seen in Fig. 1 that the diffraction pattern contains only four peaks. These peaks correspond to the ZnO hexagonal phase (sp. gr. $P6_3mc$). The X-ray peaks correspond to the (100), (002), (110), and (201) planes. In the X-ray diffraction pattern, no peaks of aluminum or aluminum oxide were observed. This is probably caused by the aluminum doping of ZnO. To estimate the average nanocrystallite size d, we used the Schererr formula $d = 0.89\lambda/\Delta(2\theta)\cos(\theta)$, where λ, θ, and $\Delta(2\theta)$ are the wavelength, Bragg angle, and full width at half maximum of the diffraction peak (rad), respectively. In this estimation, the average nanocrystallite size was ~20 nm.

According to the scanning electron microscopy study (Fig. 2), the ZnO:Al thin film surface has a nanostructured morphology consisting of nanocrystallites. Using the data from Fig. 2 and the ImageJ program, we analyzed 100 nanocrystallites along their length and width. The characteristic length and width were ~70 and ~15 nm, respectively. Here, it is worth noting that the resulting nanocrystallite width (~15 nm) is quite consistent with the average size obtained by the Schererr formula (~20 nm).

The ZnO:Al thin film surface was studied using atomic force microscopy. Figure 3 presents the image of the ZnO:Al thin film surface. It should be noted

that the ZnO:Al thin films grown by atomic layer deposition are fairly smooth and have a root-mean-square roughness of $R_q = 0.33$ nm.

The microstructure and thickness of the ZnO:Al thin films were explored by transmission electron microscopy (Fig. 4). Figure 4a shows a cross section of the ZnO:Al thin film on the glass substrate. The estimation based on Fig. 4a yielded a film thickness of ~146 nm. Figure 4b shows the electron diffraction pattern of the ZnO:Al thin film. This pattern (Fig. 4b) corresponds to the (100), (002), (101), (102), and (110) planes. The (100), (002), (110), and (201) planes were detected by both X-ray diffraction and transmission electron microscopy. It should be noted that the (201) plane is reflected on the electron diffraction pattern. The reflections from this plane are far from those of the other ZnO:Al planes in the electron diffraction pattern. In addition, the electron diffraction pattern contains the (101) and (102) planes, which were not revealed by the X-ray structural analysis. This can be due to the fact that the transmission electron microscopy study was carried out perpendicular to the ZnO : Al thin film growth plane. On the other hand, transmission electron microscopy is more sensitive than the X-ray diffraction. It is worth noting here that the peaks of aluminum or aluminum oxides were not observed either. Figure 4c shows a high-resolution image of separate ZnO:Al crystallites. One can clearly see the (002) plane with an interplanar spacing of 0.26 nm. Thus, the ZnO:Al thin films grow smooth and nanostructured without additional aluminum or aluminum oxide phases.

Figure 5 shows the dependence of the optical transmittance of the ZnO:Al thin film on the wavelength in the range of 200–2500 nm. It can be seen that the ZnO:Al thin films transmit visible light sufficiently well. The transmission at a wavelength of 550 nm with regard to the substrate was ~96%.

Figure 6 presents the spectral dependence of the refractive index n and the absorption coefficient k of the ZnO:Al thin film on a silicon substrate. It can be seen that the maximum refractive index is 2.09 at a wavelength of 335 nm. The maximum absorption coefficient was found to be 0.39 at a wavelength of 295 nm. In general, the spectral refractive indices and absorption coefficients agree quite well with the data on the ZnO:Al thin films [29, 30]. The spectral dependence of the absorption coefficient was used to estimate the optical band gap of the ZnO:Al thin films, which was determined using the formulas

$$(\alpha\hbar\nu)^2 = A(h\nu - E_g), \quad (1)$$

$$\alpha = \frac{4\pi k}{\lambda}, \quad (2)$$

where A is the proportionality coefficient, E_g is the optical band gap, $h\nu$ is the photon energy, and λ is the corresponding wavelength. The optical band gap was

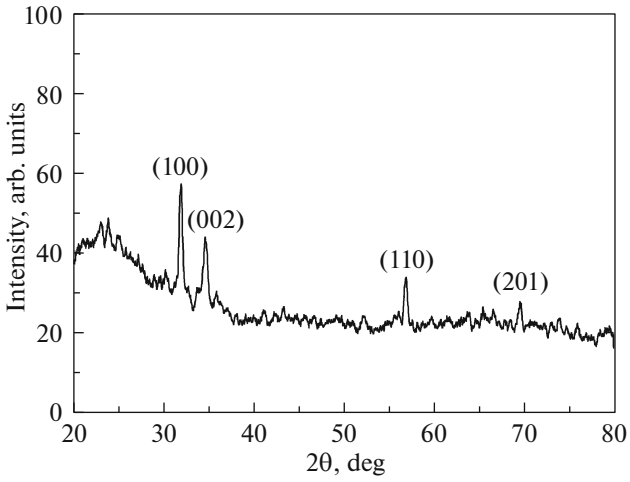

Fig. 1. X-ray diffraction data on the 146-nm-thick aluminum-doped zinc oxide thin film.

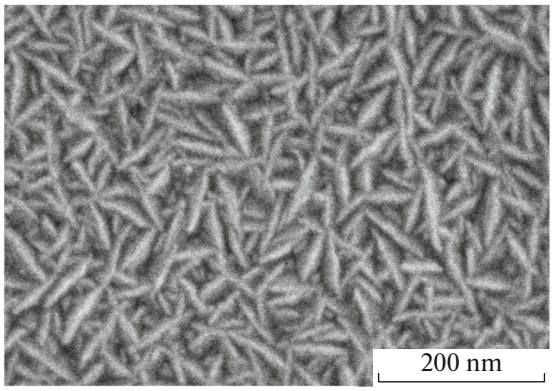

Fig. 2. Scanning electron microscopy image of the ZnO:Al film.

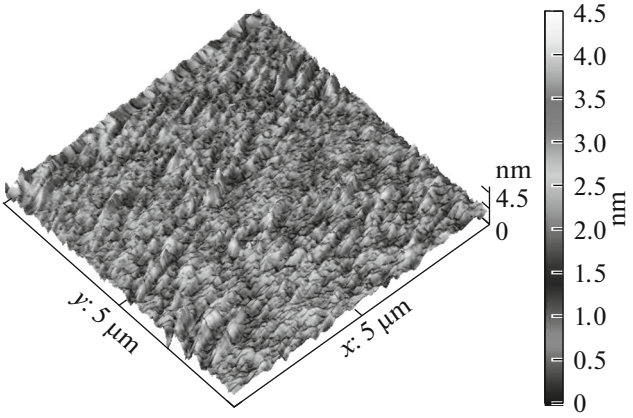

Fig. 3. Atomic force microscopy surface image of the aluminum-doped zinc oxide thin film.

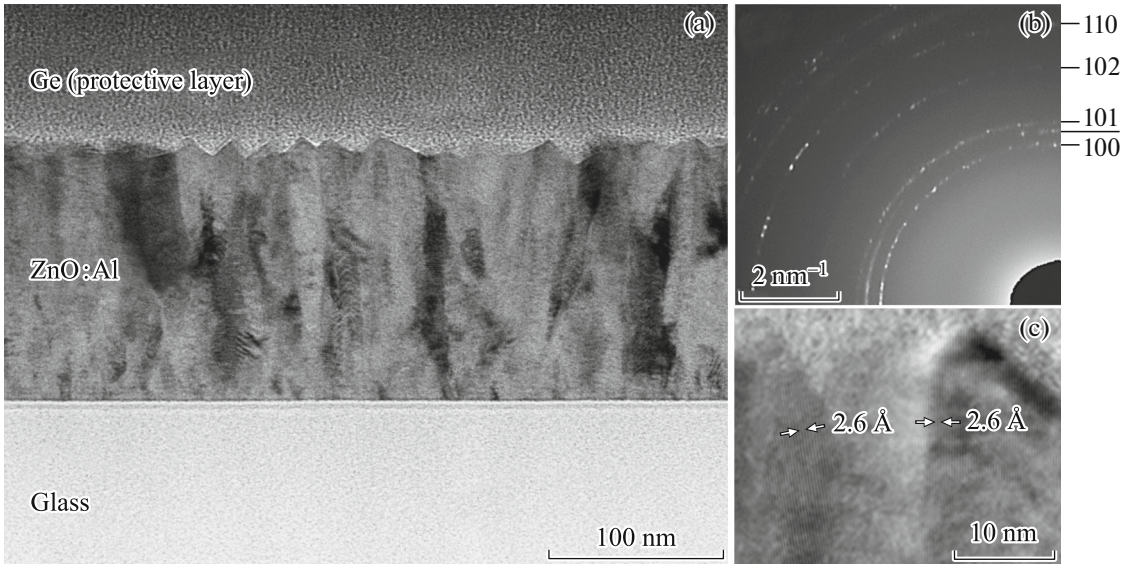

Fig. 4. (a) Transmission electron microscopy cross-sectional general view of the ZnO:Al thin film on a glass substrate, (b) the corresponding electron pattern, and (c) image of separate crystallites.

obtained by extrapolating the linear part of the $(\alpha\hbar\nu)^2$ dependence until the intersection with the abscissa axis [29, 30]. The obtained value of $E_g = 3.56$ eV is comparable with the optical band gap of the ZnO:Al thin films with the similar doping value.

In determining the thermoelectric figure of merit of a material, it is important to study its resistivity ρ as a function of temperature. To do that, we investigated the surface resistance of the ZnO:Al thin films at temperatures from room to 200°C. The surface resistance was recalculated to the resistivity over the entire film thickness. The temperature dependence of the resistivity of the ZnO:Al thin film is presented in Fig. 7. The resistivity of the ZnO:Al thin films was found to be ~1.02×10^{-3} Ω cm at room temperature. It can be seen that the resistivity decreases with increasing temperature. Such a dependence is characteristic of semiconductor materials. In [14, 31, 32], the similar temperature dependence of the resistivity of the ZnO:Al thin films was reported.

Figure 8 shows the temperature dependence of the Seebeck coefficient for the ZnO:Al thin film. The Seebeck coefficient was about −60 μV/K at room temperature and started decreasing in its absolute value with increasing temperature. The minimum absolute value of the Seebeck coefficient (~50 μV/K) was

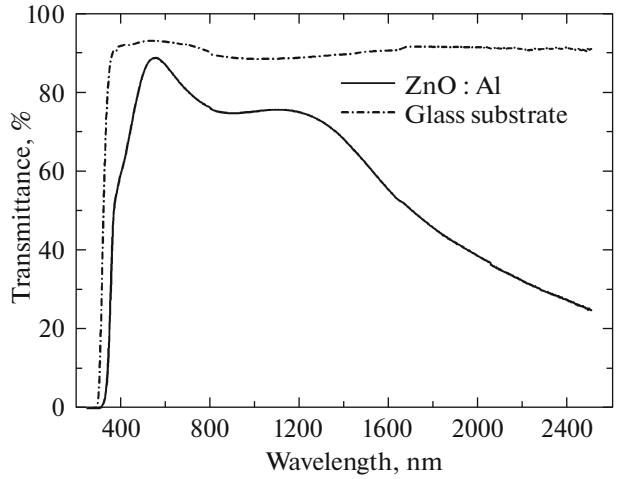

Fig. 5. Spectral dependence of transmittance of the ZnO:Al thin film.

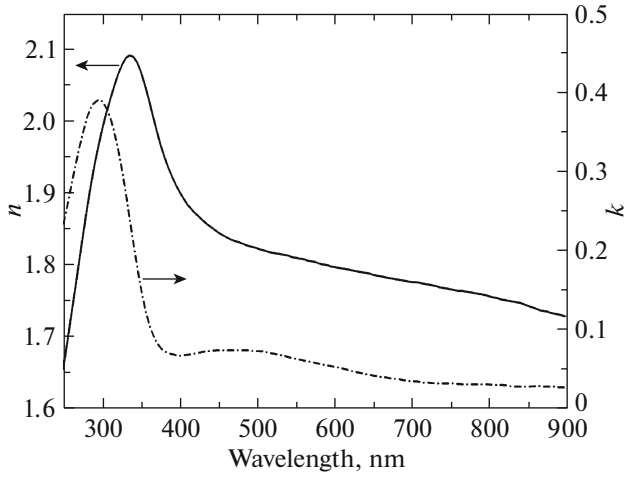

Fig. 6. Dependence of the refractive index and absorption coefficient on the wavelength for the ZnO:Al thin film on a silicon substrate.

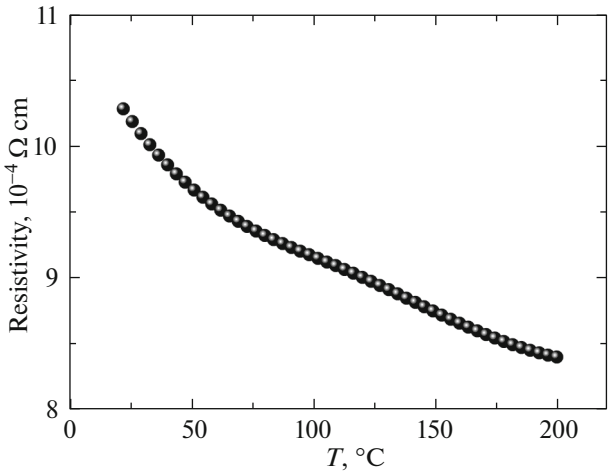

Fig. 7. Temperature dependence of the resistivity of the ZnO:Al thin film.

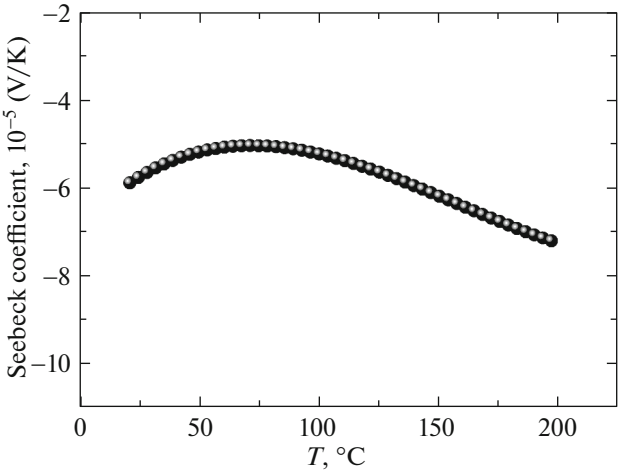

Fig. 8. Temperature dependence of the Seebeck coefficient for the ZnO:Al thin film.

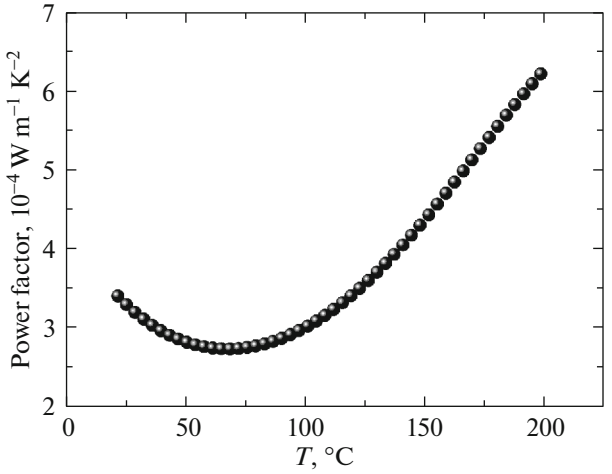

Fig. 9. Temperature dependence of the power factor of the ZnO:Al thin film.

observed at a temperature of 70°C. With an increase in temperature, starting with 70°C, the absolute value of the Seebeck coefficient increased. The maximum absolute value of the Seebeck coefficient attained ~72 μV/K at a temperature of 200°C. The obtained values of the Seebeck coefficient correspond to the values measured previously for the ZnO:Al thin films [31–33] obtained by different methods.

An important integral characteristic of thermoelectric materials is the power factor PF (μW m^{-1} K^{-2}):

$$PF = S^2\sigma. \quad (3)$$

We used formula (3), where the electrical conductivity was determined as $\sigma = 1/\rho$, to build the temperature dependence of the power factor for the ZnO:Al thin film (Fig. 9). It can be seen in Fig. 9 that the power factor of the ZnO:Al thin film decreased with an increase in temperature to ~70°C from 340–270 μW m^{-1} K^{-2}. However, with a further increase in temperature, the power factor starts increasing. The maximum power factor was 620 μW m^{-1} K^{-2} at a temperature of 200°C. The ZnO:Al thin-film samples exhibited a fairly high power factor as compared to other conductive oxides [17].

Thus, the study of the ZnO:Al thin films can be used to develop optically transparent thin-film thermoelectric converters. In addition, the obtained ZnO : Al thin films, due to their optoelectronic properties, can be used as thin-film transparent electrodes.

4. CONCLUSIONS

The ZnO:Al thin films were grown on glass and silicon substrates at a temperature of 200°C by atomic layer deposition. X-ray and electron diffraction showed that the thin films consist of the ZnO hexagonal phase. No peaks related to aluminum or aluminum oxides were observed in the X-ray and electron diffraction patterns. The ZnO:Al thin film surface has a nanostructured morphology with characteristic nanocrystallite sizes of ~70 and ~15 nm. It was found that the ZnO:Al thin films are fairly smooth and have a root-mean-square roughness of R_q = 0.33 nm. The transmittance at a wavelength of 550 nm with regard to the substrate was ~96%. In addition, the refractive indices and absorption coefficients of the ZnO:Al thin films in the wavelength range of 250–900 nm were determined. The optical band gap was found to be 3.56 eV.

The room-temperature resistivity and the Seebeck coefficient of the ZnO:Al thin films were ~1.02 × 10^{-3} Ω cm and ~60 μV/K, respectively.

The maximum absolute value of the Seebeck coefficient ~72 μV/K and the maximum power factor 620 μW m^{-1} K^{-2} were determined at a temperature of 200°C.

The ZnO:Al thin films synthesized by atomic layer deposition can be used to develop optically transpar-

ent thermoelectric converters and transparent thin-film electrodes.

ACKNOWLEDGMENTS

The electron microscopy investigations were carried out on the equipment of the Center of Collective Use of the Krasnoyarsk Scientific Center, Siberian Branch, Russian Academy of Sciences. We are grateful to F.A. Baron (Krasnoyarsk Scientific Center) for offering the opportunity of working at the growth equipment and critical discussion of the details of the sample preparation process.

FUNDING

This study was supported by the Russian Science Foundation, project no. 17-72-10079.

CONFLICT OF INTEREST

The authors declare that they have no conflicts of interest.

REFERENCES

1. X. G. Yu, T. J. Marks, and A. Facchetti, Nat. Mater. **15**, 383 (2016).
2. I. A. Tambasov, V. G. Maygkov, A. S. Tarasov, A. A. Ivanenko, L. E. Bykova, I. V. Nemtsev, E. V. Eremin, and E. V. Yozhikova, Semicond. Sci. Technol. **29**, 082001 (2014).
3. I. A. Tambasov, V. G. Myagkov, A. A. Ivanenko, I. V. Nemtsev, L. E. Bykova, G. N. Bondarenko, J. L. Mihlin, I. A. Maksimov, V. V. Ivanov, S. V. Balashov, and D. S. Karpenko, Semiconductors **47**, 569 (2013).
4. I. A. Tambasov, V. G. Myagkov, A. A. Ivanenko, L. E. Bykova, E. V. Yozhikova, I. A. Maksimov, and V. V. Ivanov, Semiconductors **48**, 207 (2014).
5. C. G. Granqvist, Sol. Energy Mater. Sol. Cells **91**, 1529 (2007).
6. P. D. C. King and T. D. Veal, J. Phys.: Condens. Matter **23**, 334214 (2011).
7. J. Keller, F. Chalvet, J. Joel, A. Aijaz, T. Kubart, L. Riekehr, M. Edoff, L. Stolt, and T. Torndahl, Prog. Photovolt. **26**, 13 (2018).
8. E. Fortunato, P. Barquinha, and R. Martins, Adv. Mater. **24**, 2945 (2012).
9. G. Korotcenkov, Mater. Sci. Eng. B **139**, 1 (2007).
10. M. Morales-Masis, F. Dauzou, Q. Jeangros, A. Dabirian, H. Lifka, R. Gierth, M. Ruske, D. Moet, A. Hessler-Wyser, and C. Ballif, Adv. Funct. Mater. **26**, 384 (2016).
11. Z. Szabo, Z. Baji, P. Basa, Z. Czigany, I. Barsony, H. Y. Wang, and J. Volk, Appl. Surf. Sci. **379**, 304 (2016).
12. A. Klein, C. Korber, A. Wachau, F. Sauberlich, Y. Gassenbauer, S. P. Harvey, D. E. Proffit, and T. O. Mason, Materials **3**, 4892 (2010).
13. O. Bierwagen, Semicond. Sci. Technol. **30**, 024001 (2015).
14. G. Luka, B. S. Witkowski, L. Wachnicki, R. Jakiela, I. S. Virt, M. Andrzejczuk, M. Lewandowska, and M. Godlewski, Mater. Sci. Eng. B **186**, 15 (2014).
15. A. Stadler, Materials **5**, 661 (2012).
16. Y. L. Liu, Y. F. Li, and H. B. Zeng, J. Nanomater. **2013**, 196521 (2013).
17. G. Korotcenkov, V. Brinzari, and M. H. Ham, Crystals **8**, 14 (2018).
18. G. J. Snyder and E. S. Toberer, Nat. Mater. **7**, 105 (2008).
19. J. He and T. M. Tritt, Science (Washington, DC, U. S.) **357**, 1369 (2017).
20. L. D. Hicks and M. S. Dresselhaus, Phys. Rev. B **47**, 12727 (1993).
21. S. Ortega, M. Ibanez, Y. Liu, Y. Zhang, M. V. Kovalenko, D. Cadavid, and A. Cabot, Chem. Soc. Rev. **46**, 3510 (2017).
22. W. Kim, J. Zide, A. Gossard, D. Klenov, S. Stemmer, A. Shakouri, and A. Majumdar, Phys. Rev. Lett. **96**, 045901 (2006).
23. C. Yang, D. Souchay, M. Kneiss, M. Bogner, M. Wei, M. Lorenz, O. Oeckler, G. Benstetter, Y. Q. Fu, and M. Grundmann, Nat. Commun. **8**, 16076 (2017).
24. T. Tynell and M. Karppinen, Semicond. Sci. Technol. **29**, 043001 (2014).
25. G. Luka, T. A. Krajewski, B. S. Witkowski, G. Wisz, I. S. Virt, E. Guziewicz, and M. Godlewski, J. Mater. Sci.-Mater. Electron. **22**, 1810 (2011).
26. I. A. Tambasov, A. S. Tarasov, M. N. Volochaev, M. V. Rautskii, V. G. Myagkov, L. E. Bykova, V. S. Zhigalov, A. A. Matsynin, and E. V. Tambasova, Phys. E (Amsterdam, Neth.) **84**, 162 (2016).
27. V. G. Myagkov, L. E. Bykova, A. A. Matsynin, M. N. Volochaev, V. S. Zhigalov, I. A. Tambasov, Y. L. Mikhlin, D. A. Velikanov, and G. N. Bondarenko, J. Solid State Chem. **246**, 379 (2017).
28. I. A. Tambasov, A. S. Voronin, N. P. Evsevskaya, M. N. Volochaev, Y. V. Fadeev, A. S. Krylov, A. S. Aleksandrovskii, A. V. Luk'yanenko, S. R. Abelyan, and E. V. Tambasova, Phys. Solid State **60**, 2649 (2018).
29. E. Ochoa-Martinez, E. Navarrete-Astorga, J. Ramos-Barrado, and M. Gabas, Appl. Surf. Sci. **421**, 680 (2017).
30. Q. H. Li, D. L. Zhu, W. J. Liu, Y. Liu, and X. C. Ma, Appl. Surf. Sci. **254**, 2922 (2008).
31. M. H. Hong, H. Choi, D. I. Shim, H. H. Cho, J. Kim, and H. H. Park, Solid State Sci. **82**, 84 (2018).
32. S. Saini, P. Mele, H. Honda, D. J. Henry, P. E. Hopkins, L. Molina-Luna, K. Matsumoto, K. Miyazaki, and A. Ichinose, Jpn. J. Appl. Phys. **53**, 060306 (2014).
33. J. T. Luo, Z. H. Zheng, G. X. Liang, F. Li, and P. Fan, Mater. Res. Bull. **94**, 307 (2017).

Translated by E. Bondareva